JOURNAL OF MATERIALS SCIENCE **40** (2005) 1953– 1958

Strain-amplitude dependent fatigue resistance of low-alloy pressure vessel steels in high-temperature water

X. Q. WU, Y. KATADA
Corrosion Resistant Design Group, Steel Research Center, National Institute for Materials Science, 1-2-1, Sengen, Tsukuba, Ibaraki, 305-0047, Japan
E-mail: WU.Xinqiang@nims.go.jp

Low cycle fatigue resistance of low-alloy pressure vessel steels was investigated in 561 K air and water over a wide strain amplitude range. It was found that fatigue resistance of the steels was enhanced in high-temperature water relative to high-temperature air under the low strain amplitude conditions (<0.3%) or in the high cycle regime ($>2 \times 10^4$ cycles), while it was remarkably degraded in high-temperature water under the higher strain amplitude conditions. Fatigue cracking and fractographic features suggested that effects of hydrogen be involved in the present corrosion fatigue process in high-temperature water. Possible environmentally assisted cracking mechanisms are discussed.

1. Introduction

High standards of safety and reliability for light water reactor (LWR) require its pressure boundary components (pressure vessel and piping system) to maintain superior integrity throughout their service lives (typically operating temperature of 561 K and design life of approximate 40 years for a boiling water reactor). During past several decades, considerable efforts have been made to investigate the environmental effects on fatigue resistance of pressure vessel steels in LWR environments [1–11], in which mechanical factors (strain rate, strain amplitude, loading waveform, ratio and frequency, etc.), environmental factors (temperature, water chemistry, flow velocity, potential, etc.), and material factors (steel or alloy compositions, heat treatments, inclusions, irradiation, etc.) were considered. It is generally accepted that LWR environments may lead to potentially significant degradation on fatigue resistance of pressure vessel steels. However, due to lack of direct experimental evidence for a specific environmentally assisted cracking (EAC) process, some aspects in this area are still under discussion, in particular the interactions between the mechanical and environmental factors.

This paper is to investigate low cycle fatigue (LCF) behavior of low-alloy pressure vessel steels in 561 K air and water and effects of strain amplitude. Possible EAC mechanisms are also discussed, in particular under the low strain amplitude condition.

2. Experimental

Low-alloy pressure vessel steels, ASTM A508 Cl.3 forging material and A533B rolling plate, were used for the present study. Chemical compositions and heat-treatments are listed in Table I. The microstructure of both steels was typical upper bainite (Fig. 1). Cylindrical LCF specimens with 8 mm gauge diameter and 16 mm gauge length were machined along the forging or rolling direction (Fig. 2). The equipments for LCF tests in high-temperature water comprised a MTS fatigue testing machine of 100 kN in dynamic load, an austenitic stainless steel autoclave of 6 liter in capacity and a water loop with 30 liter per hour flow rate. Fatigue tests were performed in an axial strain control mode with fully reversed triangular waveform. The test conditions and water chemistry are summarized in Table II. LCF life, N_{25}, was defined as the number of cycles for tensile stress to drop 25% from its peak value. Some tested specimens were broken apart in liquid nitrogen for fracture observation. A scanning electronic microscope equipped with energy dispersive X-ray spectrometry was used to examine fatigue cracking and fractographic morphologies.

3. Results

The dependence of applied strain amplitude on fatigue life in 561 K air and water for A508 Cl.3 and A533B steels are illustrated in Figs 3 and 4. Under the higher strain amplitude conditions, obvious degradation in fatigue resistance for both of steels was observed in 561 K water relative to 561 K air. This is well consistent with the general viewpoint that LWR environments may degrade the fatigue resistance of pressure vessel steels [1–11]. However, under the low strain amplitude conditions (<0.3%) or in the high cycle regime ($>2 \times 10^4$ cycles), both of steels showed relatively better fatigue resistance in 561 K water rather than in 561 K air, contrary to the general viewpoint. There seemed

TABLE I Chemical compositions and heat-treatments of A508 Cl.3[a] and A533B[b] steels

Steels	C	Si	Mn	S	P	Ni	Cr	Mo	Cu	V	Al	Fe
A508 Cl.3	0.21	0.25	1.24	0.002	0.007	0.88	0.21	0.47	0.03	0.004	0.008	Bal.
A533B	0.19	0.24	1.28	0.007	0.008	0.64	0.19	0.45	0.04	Tr.	–	Bal.

[a]1153 K × 7 h water quenched, 928 K × 9 h air cooling.
[b]1153 K × 5 h furnace cooling, 893 K × 45 h stress relief annealing.

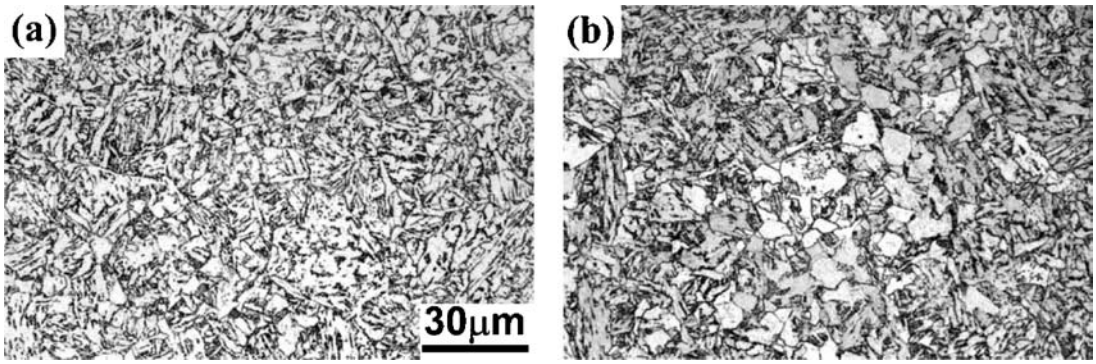

Figure 1 Optical graphs of microstructure of (a) A508 Cl.3 and (b) A533B steels used.

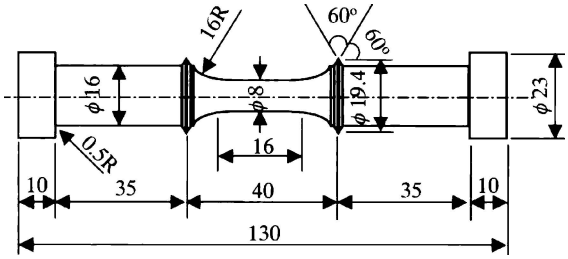

Figure 2 Illustration of LCF specimens used.

to exist a critical strain amplitude, above which high-temperature water environment degraded the fatigue resistance of both of steels, while below which the fatigue resistance in high-temperature water environment showed an anomalous enhancement compared to that in high-temperature air environment. In the present study, such a critical strain amplitude was around 0.3% for both A508 Cl.3 and A533 B steels.

The fatigue crack morphologies on specimen surfaces obtained in 561 K air and water were carefully examined. In both high-temperature air and water, similar crack morphologies were observed for both of steels. Both main and secondary cracks were zigzag with primary orientation about 45° inclined to the loading axis (Fig. 5a–c). However, in high-temperature water crack branching was frequently observed along both main and secondary cracks (Fig. 5b and c), while less crack branching could be found in high-temperature air. No significant difference in crack morphology could be observed under the different strain amplitude conditions except that less crack branching was found under

TABLE II Test conditions and water chemistry

Control mode	Strain
Wave form	Triangle
Strain rate	0.1 $\%s^{-1}$
Temperature	561 K
Pressure	8.0 MPa
Water chemistry (inlet)	
Dissolved Oxygen (DO)	0.1 ppm
pH	6.2–6.5
Conductivity	<0.2 μS/cm

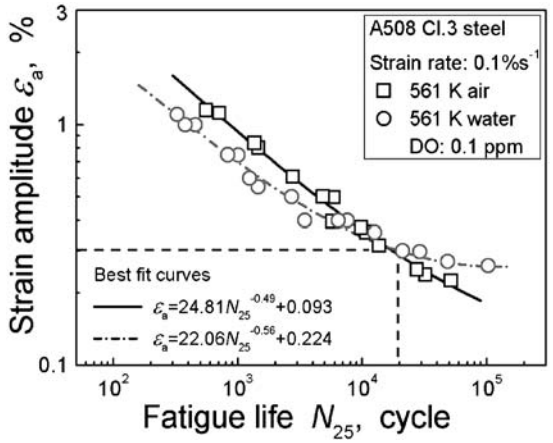

Figure 3 Dependence of applied strain amplitude on fatigue life for A508 Cl.3 steel in 561 K air and water.

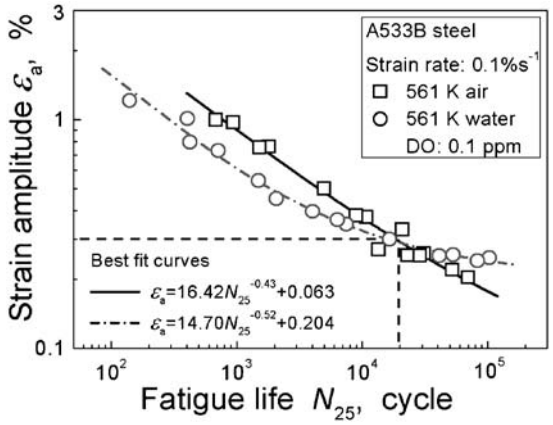

Figure 4 Dependence of applied strain amplitude on fatigue life for A533B steel in 561 K air and water.

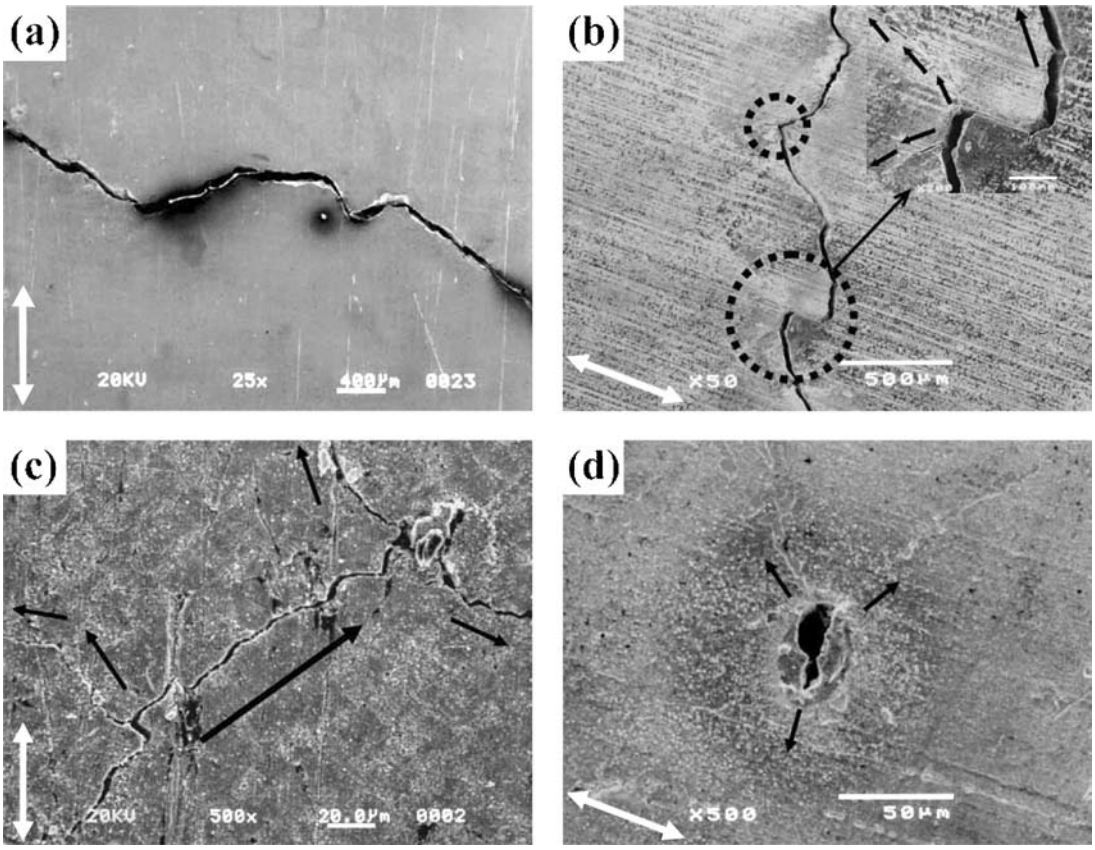

Figure 5 Fatigue crack morphologies on specimen surfaces of A508 Cl.3 steel in 561 K air and water, 0.4% strain amplitude and 0.1%s^{-1} strain rate, white arrows denote the loading axis, black arrows denote the crack propagation direction. (a) main crack in air, propagating in a zigzag manner; (b) main crack in water, propagating in a zigzag manner. The insert shows macro-crack branching in marked area; (c) secondary cracks in water and crack branching; (d) fatigue cracks initiated from a surface pit resulting from the dissolution of sulfide inclusions in water.

the low strain amplitudes. Fatigue cracks were found to initiate mainly from surface corrosion pits in high-temperature water (Fig. 5d). It is believed that formation of these corrosion pits was related to the dissolution of sulfide inclusions in spite of low solubility product k_{sp} of sulfides in water (k_{sp} is about 3.7×10^{-10} for manganese sulfide at 561 K [12]). Several pitting or cracking mechanisms assisted by sulfide dissolution have been proposed and discussed in detail in the previous literatures [2, 13–16]. In addition, fatigue cracks also initiated occasionally from subsurface inclusions.

Fig. 6 shows typical fatigue fracture morphologies obtained in 561 K air and water. Rough macro-fractures were observed for both of steels in both high-temperature air and water (Fig. 6a and c). In high-temperature air, fatigue cracks mainly initiated from subsurface inclusions (arrowed in Fig. 6a). Moreover, once a crack was initiated, it usually propagated along a fixed crack plane till final failure. When observed at a higher magnification, the fracture surface seemed to be featureless (Fig. 6b). Despite covered by oxides, slight striation-like features still remained in local areas along the crack propagation direction. In high-temperature water, however, fatigue cracks mainly initiated from surface corrosion pits resulting from the dissolution of sulfide inclusions. The crack propagation manner seemed to be much different from that in high-temperature air. The cracks usually propagated along several different crack planes rather than a fixed crack plane, involving in initiation and propagation of new cracks ahead of the original crack tips and linkage of multi-cracks on different crack planes. As a result, typical terraced morphologies accompanying secondary cracks were observed on the fracture surfaces (Fig. 6c). When observed at a higher magnification, fan-like or quasi-cleavage patterns were frequently found around the sulfide inclusions (Fig. 6d), which were very similar to the hydrogen-induced cracking features observed for hydrogen-charged steels [2, 17] or in stress corrosion cracking tests [18, 19]. Similar fractographic features could be found under the low strain amplitude conditions except for relatively slight terraced morphology and less secondary cracks.

4. Discussion

Recently, Chopra and Shack [5] have reported that a minimum strain is required for environmentally assisted decrease in fatigue lives of carbon and low-alloys steels in simulated LWR environments. This threshold value of strain amplitude for the ANL heats of carbon and low-alloy steels appears to be 0.18%, i.e., a value about 20% higher than the fatigue limit of the steels. This behavior is believed to be consistent with the film-rupture/slip-dissolution model [20] for enhancement of crack propagation, in which the applied strain must exceed a threshold value to rupture the surface passive film for environmental effects to occur. The threshold value of strain amplitude controls the crack tip strain and in turn affects the film rupture at the crack tip. In

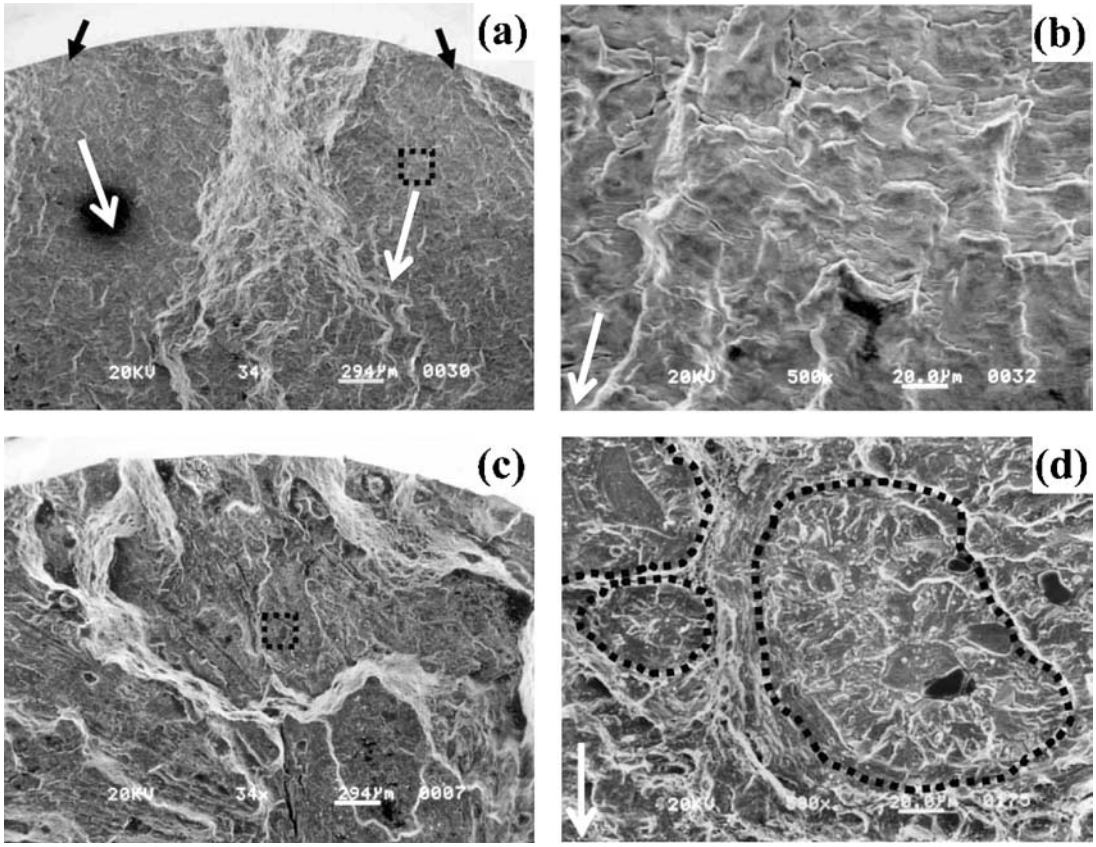

Figure 6 Fatigue fracture morphologies of A533B steel in 561 K air and water, 0.4% strain amplitude and 0.1%s^{-1} strain rate, white arrows denote the crack propagation direction. (a) in air, black arrows show crack initiation sites; (b) high magnification of marked area in (a) showing striation-like characteristic; (c) in water; (d) high magnification of marked area in (c) showing fan-like or quasi-cleavage patterns around sulfide inclusions.

the present study, there also existed a critical strain amplitude with a value of about 0.3%, above which high-temperature water environment certainly degraded the fatigue resistance of the steels, while below which the fatigue resistance in high-temperature water environment showed an anomalous enhancement compared to that in high-temperature air environment (Figs 3 and 4). However, it is rather difficult to rationalize the present experimental results only using the film-rupture/slip-dissolution model for enhancement of crack propagation. An obvious conflict is the cracking features similar to hydrogen-induced cracking observed on the fatigue fractures (Fig. 6d). The more important is the anomalous enhancement in fatigue resistance under the low strain amplitude conditions or in the high cycle regime (Figs 3 and 4).

To date, two basic mechanisms, hydrogen-assisted cracking model and film-rupture/slip-dissolution model, have been generally proposed to explain EAC behavior in LWR environments. For the former, it is suggested that hydrogen embrittlement facilitates mechanical separation at the crack tip, which is primarily based on some special cracking and fractographic features such as quasi-cleavage facets or fan-like features extending from sulfide inclusions, terraced morphology produced by linkage of hydrogen-induced cracks at sulfide-matrix interfaces ahead of the main crack, zigzag cracking accompanied by sub-cracks and macro-crack branching, etc [2, 18, 19, 21]. For the latter, it is believed that anodic dissolution of the crack-tip metal controlled the crack propagation, which is mainly supported by several theoretical models [20, 22, 23] and related experimental evidence [24–26]. Due to a lack of direct experimental evidence for a specific microscopic crack extension process, the exact EAC mechanism is therefore still under discussion. None of the proposed mechanisms can satisfactorily explain all the experimentally observed aspects of cracking. In fact, under crack-tip conditions relevant for low-alloys steels under LWR conditions, hydrogen-assisted cracking and film rupture/slip-dissolution are both thermodynamically and kinetically viable, and may therefore be simultaneously active. Since both favored mechanisms for crack propagation may depend on the same rate-determining steps such as rupture rates of oxide film, repassivation kinetics, etc., it is rather difficult to differentiate experimentally between them. In the present study, the typical cracking/fractographic features, for example, zigzag fatigue cracks and frequent crack branching (Fig. 5b and c), terraced cracking morphology and fan-like or quasi-cleavage features around sulfide inclusions (Fig. 6c and d), seemed to suggest the hydrogen-assisted cracking mechanism play a role in corrosion fatigue of low-alloy steels in high-temperature water.

It is worth noting that a better fatigue resistance under the low strain amplitude conditions (<0.3%) or in the high cycle regime ($>2 \times 10^4$ cycles) appeared in 561 K water rather than in 561 K air (Figs 3 and 4), while a distinct degradation in fatigue resistance was observed under the higher strain amplitude conditions in 561 K water. Namely, a strain-amplitude dependent fatigue

resistance appeared in high-temperature water environment. Chopra and Shack's fatigue data for A106-Gr B steel in 561 K air and water implied a similar tendency [5]. In the high cycle regime ($>10^5$ cycles), their best-fit curve for 561 K water was clearly above that for 561 K air. A similar tendency also could be found for A533-Gr B steel if extrapolating their best-fit curves to very high cycle regime (>4 or 5×10^6 cycles). Unfortunately, the exact reason for this strain-amplitude dependent fatigue resistance in high-temperature water environment, especially for the anomalous enhancement in fatigue resistance under the low strain amplitude conditions or in the high cycle regime, is not clear. If the effects of hydrogen on EAC process in high-temperature water were considered, the above cracking behavior and strain-amplitude dependent fatigue resistance may be partially rationalized.

During cyclic deformation in high-temperature water, EAC is initiated by film rupture at the crack tip due to the extrusion of slip bands. Anodic dissolution of crack-tip metal, hydrolysis of metallic cations and hydrogen reduction may take place at the bare crack tip [2]. The dissolution of sulfide inclusions at or near the crack tip is believed to promote hydrogen reduction [2, 3]. Due to its high mobility at high temperature, the hydrogen absorbed at the bare crack tip can be rapidly transported into the region of maximum hydrostatic tension ahead of the crack tip and be trapped in the inclusions/matrix or precipitation/matrix interfaces, or lath boundaries, or intersections of slip bands. Once a critical combination of hydrogen concentration and stress level is achieved, a micro-crack may initiate at these trapping sites. These micro-cracks then grow dynamically on their primary cracking planes. The growth in reversed direction may result in a linkage with the main crack tip and thus extend the main crack; however, the growth in forward direction is away from the main crack tip and may be eventually arrested because the local stress level and/or hydrogen concentration are too low to maintain the growth. Because the primary cracking planes of these micro-cracks are not fixed and may be different from that of the main crack, the fatigue cracks grow in a zigzag manner accompanying frequent crack branching and typical terraced fracture surfaces and hydrogen-assisted cracking features are obtained correspondingly (Figs 5b, c and 6c, d).

The applied strain amplitude is believed to affect the above hydrogen-assisted EAC. At the same strain rates, both film-rupture rate at the crack tip and maximum tensile stress ahead of the crack tip under the low strain amplitude conditions are relatively low compared to the high strain amplitude cases. This is unfavorable to the absorption of hydrogen at the crack tip and the transportation of hydrogen into the cyclic plastic zone ahead of the crack tip. The hydrogen concentration in the plastic zone thus keeps a lower value compared to the high strain amplitude cases and the hydrogen-assisted brittle cracking effects may be retarded to some extent. Moreover, it should be noted that the present fatigue tests were performed in a total strain control mode. In high-temperature water, the hydrogen-affected crack-tip metal would have a lower cyclic stress amplitude compared to the hydrogen-free case (in high-temperature air) under the same cyclic strain amplitude condition due to the effects of hydrogen-induced softening [17]. This is believed to partially contribute to the better fatigue resistance under the low strain amplitude conditions or in the high cycle regime in 561 K water. Another possible factor may be related to the crack closure induced by corrosion products in high-temperature water environment. The low applied strain amplitude induces a low film-rupture rate at the crack tip under the same strain rate condition. The film (both oxide and other corrosion product films) may reduce the effective stress strength factor range at the crack tip through reducing the crack tip opening displacement, and thus enhance the crack closure, by which the fatigue crack growth rate is reduced. Similar crack closure effects have been reported to play significant roles in the behavior of small cracks or at the stage of near-threshold growth stage [27, 28]. In this regard, the corrosion-product-induced crack closure may partially contribute to the better fatigue resistance under the low strain amplitude conditions or in the high cycle regime in 561 K water.

5. Conclusions

Under the low strain amplitude conditions ($<0.3\%$) or in the high cycle regime ($>2 \times 10^4$ cycles), an enhancement in fatigue resistance was observed for low-alloy pressure vessel steels in 561 K water relative to 561 K air, while under the higher strain amplitude conditions, obvious degradation in fatigue resistance was observed in 561 K water. The fatigue cracking and fractographic features suggested that hydrogen effects play a role in the present corrosion fatigue process of low-alloy pressure vessel steels in high-temperature water. The above strain-amplitude dependent fatigue resistance may be partially attributed to hydrogen-induced decrease in cyclic stress amplitude and corrosion-product-induced crack closure.

Acknowledgments

This study was financially supported by the Budget for Nuclear Research of Japanese Ministry of Education, Culture, Sports, Science and Technology, based on the screening and counseling by the Atomic Energy Commission.

References

1. T. KONDO, T. KIKUYAMA, H. NAKAJIMA, M. SHINDO and R. NAGASAKI, *Nucl. Eng. Des.* **17** (1971) 170.
2. H. HÄNNINEN, K. TÖRRÖNEN, M. KEMPPAINEN and S. SALONEN, *Corros. Sci.* **23** (1983) 663.
3. N. NAGATA, S. SATO and Y. KATADA, *ISIJ Intern.* **31** (1991) 106.
4. M. HIGUCHI, K. IIDA and Y. ASADA, *ASTM STP* **1298** (1997) 216.
5. O. K. CHOPRA and W. J. SHACK, *Nucl. Eng. Des.* **184** (1998) 49.
6. S. G. LEE and I. S. KIM, *J. Press. Vess. Technol. Trans. ASME* **123** (2001) 173.
7. J. CONGLETON, E. A. CHARLES and G. SUI, *Corros. Sci.* **43** (2001) 2265.

8. O. K. CHOPRA and W. J. SHACK, *ASME PVP* **453** (2003) 71.
9. A. HIRANO, M. YAMAMOTO, K. SAKAGUCHI, T. SHOJI and K. IIDA, *J. Press. Vess. Technol. Trans. ASME* **125** (2003) 403.
10. X. Q. WU and Y. KATADA, *J. Mater. Sci.* **39** (2004) 2519.
11. *Idem.*, *Mater. Sci. Eng.* **379A** (2004) 58.
12. S. LICHT, *J. Electrochem. Soc.* **135** (1988) 2971.
13. G. WRANGLEN, *Corros. Sci.* **14** (1974) 331.
14. J. H. BULLOCH, *Int. J. Press. Vess. Piping* **56** (1993) 149.
15. X. Y. ZHOU, J. CONGLETON and A. BAHRALOLOOM, *Corrosion* **54** (1998) 898.
16. Y. KATADA and K. KUROSAWA, *ASME PVP* **386** (1999) 249.
17. X. Q. WU and I. S. KIM, *Mater. Sci. Eng.* **348A** (2003) 309.
18. H. HÄNNINEN, W. CULLEN and M. KEMPPAINEN, *Corrosion* **46** (1990) 563.
19. J. KUNIYA, H. ANZAI and I. MASAOKA, *ibid.* **48** (1992) 419.
20. F. P. FORD, *ibid.* **52** (1996) 375.
21. J. D. ATKINSON and J. YU, *Fat. Fract. Eng. Mater. Struct.* **20** (1997) 1.
22. P. M. SCOTT and A. E. TRUSWELL, *J. Press. Vess. Technol. Trans. ASME* **105** (1983) 245.
23. P. S. MAIYA, *ibid.* **109** (1987) 116.
24. P. M. SCOTT, A. E. TRUSWELL and S. G. DRUCE, *Corrosion* **40** (1984) 350.
25. D. J. GAVENDA, P. R. LUEBBERS and O. K. CHOPRA, *Fat. Fract. J.* **350** (1997) 243.
26. O. K. CHOPRA and W. J. SHACK, *J. Press. Vess. Technol. Trans. ASME* **121** (1999) 49.
27. A. SAXENA, in "Nonlinear Fracture Mechanics for Engineer" (CRC Press, New York, 1998) p. 303.
28. S. SURESH, G. F. ZAMISKI and R. O. RITCHIE, *Metall. Trans.* **12A** (1981) 1435.

Received 13 September
and accepted 24 September 2004